



A THEORY OF DISLOCATION CELL FORMATION BASED ON STOCHASTIC DISLOCATION DYNAMICS

P. HÄHNER

Joint Research Centre of the European Commission, Institute for Advanced Materials, T.P 750, I-21020 Ispra (Va), Italy

(Received 10 August 1995; in revised form 28 August 1995)

Abstract—A stochastic effective medium theory is developed that accounts for the geometrically necessary fluctuations of the local stress and strain rate resulting from dynamic dislocation interactions. The concept is applied to the formation of dislocation cells in multiple slip. Starting from a Langevin-type evolution equation for the total dislocation density ρ , a corresponding Fokker–Planck equation for the probability distribution $p_s(\rho)$ is derived. Cell formation is related to a noise-induced non-equilibrium phase transition associated with a qualitative change of $p_s(\rho)$. The cell size is found to be in inverse proportion to the flow stress (principle of similitude). Critical conditions for, and the role of cross slip in, cell formation are discussed.

1. INTRODUCTION

Plastic deformation of metals may give rise to the formation of cellular dislocation structures that consist of regions of low dislocation density (cell interiors) separated by dense dislocation entanglements (cell walls) [1–3]. In multiple-slip oriented face-centered cubic (f.c.c.) single crystals and f.c.c. polycrystals, cell structures emerge readily with increasing strain in the entire range of deformation temperatures. For single-slip orientations, dislocation patterning commences at the end of stage II by the development of heterogeneous entanglements, while pronounced cell formation is related to the onset of stage III, indicating that cell structures are facilitated by the cross slip of screw dislocations. A different situation is observed with body-centered cubic (b.c.c.) metals during low temperature deformation, where dislocation arrangements remain more or less homogeneous even at large strains, whereas cell structures develop above the transition temperature [4].

Although cell structures occur in a wide range of materials deformed under various conditions, their appearance seems to obey universal principles. This is reflected by the validity of empirical scaling laws relating the cell size λ , the total dislocation density ρ and the tensile flow stress σ^{ext} . The relationship between λ and σ^{ext} (“principle of similitude” [5]) is expressed as

$$\frac{\lambda}{b} = K_1 \left(\frac{\mu}{\sigma^{\text{ext}}} \right)^m \quad (1)$$

where b is the length of the Burgers vector and μ is the shear modulus. As a compilation of available data [6] shows, $K_1 \approx 20$ and $m \approx 1$ constitute a master

curve for most materials (both f.c.c. and high-temperature deformed b.c.c. metals). There are, however, exceptions with m smaller than 0.5 or larger than 1.5, the physical (or metrological?) origins of which are unclear [6]. The cell size, λ , is in proportion to the average dislocation spacing [6]

$$\lambda = K_2 \rho^{-1/2}, \quad (2)$$

which is equivalent to equation (1), if a flow stress rule [7]

$$\sigma^{\text{ext}} = \tilde{\alpha} \mu b \rho^{1/2} \quad (3)$$

is assumed, with $m = 1$ and a coefficient $\tilde{\alpha} = K_1/K_2$ of the order of unity.

Various models of dislocation patterning have been proposed that differ right from the starting point, namely the driving force of this process. According to the thermodynamic approach, dislocation cells are considered a consequence of the second law of thermodynamics (“low energy dislocation structures”): “During straining, dislocations are trapped mutually and it must be expected that such interactions would follow the general principle of minimization of free energy . . . [5]”. For a specific application of this idea, the structure was assumed to consist of a checkerboard pattern of cells with alternating sense of misorientation, and the dislocation energy (self-energy plus interaction energy) was minimized with respect to the cell size. This gives a possible explanation of the experimentally established scaling relations (1) and (2) [5]. The thermodynamic approach is, however, problematic, as energy minimization principles do not apply to dissipative processes far from equilibrium, such as dislocation glide during plastic deformation. For the

same reason, the model of dislocation patterning proposed by Holt [8] is not fully convincing, as it is based on a close-to-equilibrium generalization in terms of linear irreversible thermodynamics.

In synergetic theories of dislocation patterning the far-from-equilibrium nature of plastic flow is properly accounted for by considering the nonlinear dynamics of various dislocation densities, such as mobile, immobile and dipole dislocation configurations. The highly developed models by Walgraef and Aifantis [9] and Kratochvil [10] focus on the evolution and dynamic stability of dipolar dislocation arrangements. An inherent weakness of current synergetic models relates to the neglect of long-range dislocation interactions. This could be a problem with dislocation cell formation where patterning occurs on the same mesoscopic length scale that governs the effective range of dislocation interactions.

Although cell formation has been comprehensively investigated both from the experimental and from the theoretical side, three major aspects are not fully understood. (i) What is the driving force of dislocation patterning in general; (ii) what are the material properties and testing conditions required specifically for cell formation; and (iii) what is the physical significance of the scaling parameters K_1 and K_2 [equations (1) and (2)]? In the present paper, these questions shall be addressed by starting from the observation that cell formation is a collective dislocation effect in multiple slip (forest patterning [1, 2]). The new element of the following analysis is a stochastic dislocation dynamics suitable for accounting for the effect of long-range dislocation interactions on a mesoscopic scale. The general ideas of this approach are outlined in Section 2, while a detailed application to the present problem is developed in Section 3. Sections 4 and 5 present a discussion of results and some general conclusions, respectively.

2. STOCHASTIC DISLOCATION DYNAMICS

Long-range dislocation interactions are known to play an important role in dislocation dynamics, in particular, when collective phenomena occur: strain localization, dislocation patterning, plastic instabilities. Instead of treating the microscopic details (which is, of course, impossible in analytical modelling), we shall proceed by considering a mesoscopic statistical equivalent of dislocation interactions. To this end, we express the effective shear stress τ^{eff} (the driving stress acting on a glide dislocation) by the external resolved shear stress τ^{ext} , and the long-range internal shear

stress τ^{int} (the back stress caused by other dislocations)

$$\tau^{\text{eff}} = \tau^{\text{ext}} - \tau^{\text{int}}. \quad (4)$$

During its glide motion, a mobile dislocation interacts with various dislocation configurations so that it experiences fluctuations of the effective stress

$$\delta\tau^{\text{eff}} = -\delta\tau^{\text{int}}. \quad (5)$$

For a determination of the intensity of the effective stress fluctuations and the corresponding strain-rate fluctuations, consider a representative mobile dislocation gliding at a velocity v (that also fluctuates with time) and calculate

$$\langle v\tau^{\text{int}} \rangle = \frac{1}{\Delta t} \int_0^{\Delta t} dt v \tau^{\text{int}} = \frac{1}{\Delta x} \int_0^{\Delta x} dx \tau^{\text{int}} = 0. \quad (6)$$

Here, $\langle \dots \rangle$ denotes a temporal average effected over a sufficiently long interval of time Δt during the glide motion of the representative dislocation. Note that with $dx = v dt$ the temporal average is transformed into a spatial average of the internal stress that vanishes,† provided that averaging can be performed over a distance Δx that is long compared to the characteristic scale of the variations of the internal stress. This necessitates the slip line length to be much longer than the dislocation spacing.

Since equation (6) applies to any representative glide dislocation, a corresponding relation holds for the local plastic shear strain rate $\dot{\gamma}$:

$$\langle \dot{\gamma}\tau^{\text{int}} \rangle = 0 \text{ or } \langle \dot{\gamma}\tau^{\text{eff}} \rangle = \langle \dot{\gamma} \rangle \tau^{\text{ext}}. \quad (7)$$

This is a mesoscopic continuum formulation which requires that the average dislocation spacing is small compared with the correlation length of fluctuations [cf. equation (15)]. Equation (7) states that the contribution of the internal stresses to the mechanical power density is completely dissipative. It represents an approximate result, because dislocation reactions may impede the glide dislocations to scan a sufficient manifold of internal stress configurations. However, as a refined treatment accounting for the influences of dislocation multiplication, storage and cross slip [11] shows, equation (7) is a good approximation for the following analysis.

From equations (4) and (7) cross-correlations of $\dot{\gamma}$ and τ^{eff} fluctuations derive if one notes that $\tau^{\text{ext}} = \text{const.}$ on the time scale of dislocations interactions:

$$\langle \delta\dot{\gamma}\delta\tau^{\text{eff}} \rangle = \langle \dot{\gamma}\tau^{\text{eff}} \rangle - \langle \dot{\gamma} \rangle \langle \tau^{\text{eff}} \rangle = \langle \dot{\gamma} \rangle \langle \tau^{\text{int}} \rangle. \quad (8)$$

The auto-correlations (fluctuation intensities) of the strain-rate and the effective stress are readily obtained by introducing the strain-rate sensitivity

$$S = \frac{\partial \langle \tau^{\text{eff}} \rangle}{\partial \ln \langle \dot{\gamma} \rangle} \quad (9)$$

which represents the response function appropriate to convert strain-rate fluctuations into effective stress fluctuations and vice versa. Neglecting higher than

†This is an immediate consequence of quasi-static stress equilibrium which, in 2D, is sometimes referred to as Albenga's rule. The temporal average $\langle \tau^{\text{int}} \rangle$, however, is positive, as a glide dislocation spends most of the time at positions with positive back stress.

second order correlations, this gives

$$\langle \delta \dot{\gamma}^2 \rangle = \frac{\langle \tau^{\text{int}} \rangle}{S} \langle \dot{\gamma} \rangle^2 \quad (10)$$

and

$$\langle (\delta \tau^{\text{eff}})^2 \rangle = S \langle \tau^{\text{int}} \rangle. \quad (11)$$

Equations (10) and (11) may be called “fluctuation–dissipation theorems of plastic flow”, as they relate the local fluctuations of strain rate and effective stress to the response function S and the mechanical power dissipation. These fluctuations represent an intrinsic phenomenon of plastic deformation by dislocation glide, as they are geometrically necessary when dislocations are forced to glide across each other. It is interesting to note that an important role in the plastic deformation behavior is assigned to the strain-rate sensitivity S . In strongly rate-sensitive b.c.c. metals, stress fluctuations are predicted to be comparatively large (stress concentrations), while strain-rate fluctuations are small (homogeneous flow). The opposite trend holds for f.c.c. metals, where S is small and where correspondingly large relative strain-rate fluctuations are predicted,

$$\frac{\langle \delta \dot{\gamma}^2 \rangle}{\langle \dot{\gamma} \rangle^2} = \frac{\langle \tau^{\text{int}} \rangle}{S} \approx 10 \dots 10^3, \quad (12)$$

which can be attributed to collective dislocation glide in groups of

$$n = (2\pi)^{1/4} \sqrt{\frac{\langle \tau^{\text{int}} \rangle}{S}} \approx 5 \dots 50 \quad (13)$$

dislocations (formation of slip lines) [11].

To complete the theoretical framework, estimates for the spatial and temporal correlations are needed. Assuming that glide dislocations move in groups and, therefore, experience correlated deviations from the average effective stress all during the time passing between generation and storage (or annihilation), we get the following scaling law for the correlation time

$$\tau = \frac{b\rho_m L}{\langle \dot{\gamma} \rangle}. \quad (14)$$

Here ρ_m is the density of mobile dislocations, and L is the slip line length.

As an immediate consequence of the reciprocal distance interaction law, dislocations arranged at random within an infinite medium possess an infinite interaction range [12]. This is why the physical significance of a correlation length is not obvious. From the dynamic point of view, however, it can be defined by noting that stress fluctuations tend to destroy the dislocation correlations. Hence, two dislocations are expected to behave collectively, only if their inter-

action stress exceeds the stress fluctuations caused by other dislocations of the surroundings. This is expressed by a scaling law for the correlation length

$$\xi = \frac{\mu b}{4\pi \sqrt{\langle (\delta \tau^{\text{eff}})^2 \rangle}} = \frac{\mu b}{4\pi \sqrt{S \langle \tau^{\text{int}} \rangle}}. \quad (15)$$

Note that, while playing the role of a cut-off for dislocation interactions similar to what was postulated in Holt's work [8], the present correlation length is of dynamic origin.

The central idea behind a stochastic dislocation dynamics concept is considering dislocation glide to occur embedded into an *effective fluctuating medium* made up by the residual dislocations. Equations (10), (11), (14) and (15), though partly phenomenological in nature, are supposed appropriate for seizing the mesoscopic aspects of long-range interactions. We shall set up a simple model of dislocation cell formation to show that the stochastic dislocation dynamics allows for deriving new types of relationships that cannot be obtained from a deterministic line of reasoning.

3. FORMULATION

3.1. Constitutive equations

Consider a $\langle 100 \rangle$ oriented crystal with f.c.c. (b.c.c.) structure with eight equivalent $\langle 110 \rangle \{111\}$ ($\langle 111 \rangle \{110\}$) glide systems operating during tensile straining [13]. As statistically isotropic dislocation structures develop in this case, we proceed on a scalar formulation in terms of the coupled evolution of the densities ρ_m and ρ_i of mobile and immobile dislocations, respectively. The constitutive equations to be employed account for dislocation multiplication, storage and annihilation:

$$\partial_t \rho_m = A \tau^{\text{eff}} \dot{\gamma} - B_1 \sqrt{\rho} \dot{\gamma} - \frac{B_2}{2} \sqrt{\rho} \dot{\gamma}, \quad (16)$$

$$\partial_t \rho_i = B_1 \sqrt{\rho} \dot{\gamma} - \frac{B_2}{2} \sqrt{\rho} \dot{\gamma} \quad (17)$$

where $\rho = \rho_m + \rho_i$ denotes the total dislocation density and A , B_1 and B_2 are parameters. The first term on the right-hand side (r.h.s.) of equation (16) stands for dislocation multiplication, either by dislocations bowing out when the local effective stress exceeds the critical Orowan stress, or by the operation of a Frank–Read source after double cross-slip of a screw dislocation. The parameter A that was estimated [14] to be $A \approx 0.1/(\mu b^2)$ will be adjusted to strain-hardening (Section 4). The second term on the r.h.s. of equation (16) and the corresponding term of equation (17) describe the immobilization of dislocations (storage in the dislocation network). Finally, the last term of equations (16) and (17), respectively, accounts for the glide-induced dislocation annihilation with a coefficient $B_2 < B_1$. As this process is facilitated by cross slip, B_2 may increase with strain, while B_1 decreases, owing to an enhanced dynamic recovery by cross slip (cf. Section 4).†

†Kocks [15] proposed to describe dislocation annihilation by a loss term $(-B\rho\dot{\gamma})$. A $\sqrt{\rho}$ dependence, however, seems more appropriate, as both the annihilated dislocation lengths and the annihilation distance are expected to scale with the characteristic dimension of the dislocation network, i.e. $\rho^{-1/2}$.

Taking the sum of equations (16) and (17) gives the evolution of the total dislocation density

$$\partial_t \rho = A \tau^{\text{eff}} \dot{\gamma} - B_2 \sqrt{\rho} \dot{\gamma}. \quad (18)$$

When this is considered a *deterministic* evolution equation, it does not possess any peculiarities characteristic of dislocation cell formation. This is readily confirmed by making some assumption on the ρ dependence of τ^{eff} and integrating equation (18) by separation of variables. If it is, however, interpreted as a *stochastic* differential equation, qualitatively new features arise due to the fluctuations of the effective stress and the strain rate.

If τ^{eff} and $\dot{\gamma}$ are allowed to fluctuate, equation (18) reads

$$\partial_t \rho = A(\langle \tau^{\text{eff}} \dot{\gamma} \rangle + \langle \tau^{\text{eff}} \rangle \delta \dot{\gamma} + \langle \dot{\gamma} \rangle \delta \tau^{\text{eff}} - B_2 \sqrt{\rho} (\langle \dot{\gamma} \rangle + \delta \dot{\gamma})). \quad (19)$$

Here $\delta \dot{\gamma}$, $\delta \dot{\gamma}'$ and $\delta \tau^{\text{eff}}$ are random increments of $\dot{\gamma}$ and τ^{eff} , respectively, and a second-order stochastic term was approximated by

$$\delta \tau^{\text{eff}} \delta \dot{\gamma} \approx \langle \delta \tau^{\text{eff}} \delta \dot{\gamma} \rangle = \langle \tau^{\text{eff}} \dot{\gamma} \rangle - \langle \tau^{\text{eff}} \rangle \langle \dot{\gamma} \rangle. \quad (20)$$

To proceed further, we combine the various fluctuating terms of equation (19) by making the following assumptions. (i) $\delta \tau^{\text{eff}}$ and $\delta \dot{\gamma}$ are in phase, as the strain rate responds instantaneously to the effective stress ($\delta \tau^{\text{eff}} = S \delta \dot{\gamma} / \langle \dot{\gamma} \rangle$). (ii) Multiplication is enhanced when annihilation is reduced and vice versa ($\delta \dot{\gamma} = -\delta \dot{\gamma}'$). This corresponds to the occurrence of "weak zones" in the dislocation network. Moreover, it is convenient to introduce dimensionless variables $\tilde{\rho}$ and \tilde{t} according to

$$\rho = c_1 \tilde{\rho} \text{ with } c_1 = \left(\frac{A \langle \tau^{\text{eff}} \dot{\gamma} \rangle}{B_2 \langle \dot{\gamma} \rangle} \right)^2 \quad (21)$$

and

$$t = c_2 \tilde{t} \text{ with } c_2 = \frac{A \langle \tau^{\text{eff}} \dot{\gamma} \rangle}{(B_2 \langle \dot{\gamma} \rangle)^2}, \quad (22)$$

and to replace $\delta \dot{\gamma}$ by a standard correlated stochastic process δW by scaling

$$\delta \dot{\gamma} = \sqrt{2\tilde{\tau} \langle \delta \dot{\gamma}^2 \rangle} \delta W, \quad (23)$$

with

$$\tilde{\tau} = \frac{\tau}{c_2} \quad (24)$$

†Two calculi for the derivation of the FPE are known in the literature: the (i) Ito and (ii) Stratonovich calculus [16, 17]. They differ with respect to the definition of the differential time increments used in the evaluation of the stochastic integrals. This is by no means trivial, as another infinitesimally short time scale was introduced by the white noise approximation, equation (28). For the present case, the Stratonovich calculus seems more appropriate, since equation (29) was derived as a white-noise limit of a physical noise spectrum [16]. In any case, the following results and conclusions are not qualitatively affected by this choice.

being the dimensionless correlation time [cf. equations (14) and (22)]. Using equations (20)–(24), (19) can be written in the compact form

$$\partial_t \tilde{\rho} = 1 - \sqrt{\tilde{\rho}} + \sigma(\phi + \sqrt{\tilde{\rho}}) \delta W. \quad (25)$$

It should be noted that this is a generalized Langevin equation that was formed phenomenologically for describing the evolution of the total dislocation density in multiple slip. The r.h.s. of equation (25) consists of three qualitatively different contributions. The first two terms describe the systematic evolution [c.f. the deterministic interpretation of equation (18)], while the term proportional to

$$\phi = \frac{\langle \tau^{\text{eff}} \rangle + S}{\tau^{\text{ext}}} \quad (26)$$

represents the so-called *additive* noise (i.e. a fluctuating term the prefactor of which is a smooth average value). In contrast to this, the last term ($\sigma \sqrt{\tilde{\rho}} \delta W$) is a *multiplicative* noise depending on the stochastic variable ρ . As we shall see below, this term can produce a noise-induced transition [16]. The noise intensity parameter σ^2 reads

$$\sigma^2 = \tilde{\tau} \frac{\langle \delta \dot{\gamma}^2 \rangle}{\langle \dot{\gamma} \rangle^2} = \tilde{\tau} \frac{\langle \tau^{\text{int}} \rangle}{S}. \quad (27)$$

With typical experimental parameter values (cf. Section 4), $\tilde{\tau}$ turns out to be small compared to the characteristic time of the systematic evolution ($\tilde{\tau} \ll 1$). The noise can therefore be approximated by a Gaussian white noise process characterized by

$$\langle \delta W(0) \delta W(\tilde{t}) \rangle = \delta(\tilde{t}) \quad (28)$$

where $\delta(\tilde{t})$ denotes Dirac's delta function. This is a formal consequence of the fact that the geometrically necessary fluctuations of stress and strain rate are fast compared to the macroscopic evolution of the dislocation density.

3.2. Fokker–Planck equation and probability density

The Langevin equation (25) possesses the form

$$\partial_t \tilde{\rho} = f(\tilde{\rho}) + \sigma g(\tilde{\rho}) \delta W, \quad (29)$$

with

$$f(\tilde{\rho}) = 1 - \sqrt{\tilde{\rho}} \text{ and } g(\tilde{\rho}) = \phi + \sqrt{\tilde{\rho}}. \quad (30)$$

Standard methods can be applied for deriving a Fokker–Planck equation (FPE) for the corresponding probability distribution. Using the Stratonovich calculus [16, 17] this yields:†

$$\partial_{\tilde{t}} p = -\partial_{\tilde{\rho}} \left[\left(f(\tilde{\rho}) + \frac{\sigma^2}{2} g(\tilde{\rho}) \partial_{\tilde{\rho}} g(\tilde{\rho}) \right) p \right] + \frac{\sigma^2}{2} \partial_{\tilde{\rho}}^2 [g^2(\tilde{\rho}) p] \quad (31)$$

where $p = p(\tilde{\rho}, \tilde{t} | \tilde{\rho}_0, \tilde{t}_0)$ denotes the transition probability density from a state $(\tilde{\rho}_0, \tilde{t}_0)$ to $(\tilde{\rho}, \tilde{t})$. Due to the slow systematic evolution of the system, the stochastic process may be approximated by a stationary one, i.e. the transition probability density is time homogeneous:

$$p(\tilde{\rho}, \tilde{t} + \tilde{t}' | \tilde{\rho}_0, \tilde{t}') = p(\tilde{\rho}, \tilde{t} | \tilde{\rho}_0, 0). \quad (32)$$

For the same reason, fluctuation amplitudes adjust quasi-instantaneously to the macroscopic evolution. Under these circumstances, all information pertinent to the stochastic dynamics of the system is obtained from the steady-state solution of equation (31), that is the stationary probability density

$$\begin{aligned} p_s(\tilde{\rho}) &= \frac{N}{g(\tilde{\rho})} \exp \left[\frac{2}{\sigma^2} \int_0^{\tilde{\rho}} d\tilde{\rho}' \frac{f(\tilde{\rho}')}{g^2(\tilde{\rho}')} \right] \\ &= N' (\phi + \sqrt{\tilde{\rho}})^{4(1+2\phi)/\sigma^2 - 1} \\ &\quad \times \exp \left[-\frac{4}{\sigma^2} \sqrt{\tilde{\rho}} + \frac{4}{\sigma^2} \frac{\phi(\phi+1)}{(\phi + \sqrt{\tilde{\rho}})} \right]. \end{aligned} \quad (33)$$

N and N' are normalization constants chosen in a way that

$$\int_0^\infty d\tilde{\rho} p_s(\tilde{\rho}) = 1. \quad (34)$$

In the following, equation (33) shall be used to explore the possibility of a noise-induced transition related to the formation of dislocation cells. Such a transition can be associated with a qualitative change of the steady-state distribution $p_s(\tilde{\rho})$ owing to the appearance or disappearance of an extremum when the control parameters ϕ and σ^2 reach critical values.

The extremum condition

$$\partial_{\tilde{\rho}} p_s(\tilde{\rho}) = 0 \quad (35)$$

gives

$$f = \frac{\sigma^2}{2} g \partial_{\tilde{\rho}} g \quad (36)$$

or

$$x^2 + \left(\frac{\sigma^2}{4} - 1 \right) x + \frac{\sigma^2}{4} \phi = 0 \quad \text{with } x = \sqrt{\tilde{\rho}} \geq 0, \quad (37)$$

the solutions of which are

$$x_{\pm} = \frac{1}{2} \left(1 - \frac{\sigma^2}{4} \right) \pm \sqrt{\frac{1}{4} \left(1 - \frac{\sigma^2}{4} \right)^2 - \frac{\sigma^2}{4} \phi}. \quad (38)$$

Two extrema $x_{\pm} > 0$ exist if the discriminant is

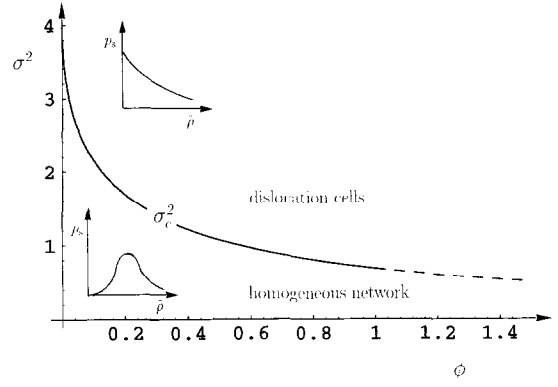


Fig. 1. Phase diagram of dislocation cell formation. The phase boundary $\sigma_c^2(\phi)$ separates the regions of peaked and monotonically decreasing probability distribution functions, respectively.

positive, i.e. for:

$$\sigma^2 < \sigma_c^2 = 4[1 + 2\phi - 2\sqrt{\phi(\phi+1)}]. \quad (39)$$

As shown in the phase diagram, Fig. 1, the critical noise intensity σ_c^2 is decreasing with increasing additive noise parameter ϕ . For $\sigma^2 < \sigma_c^2$, x_+ represents a maximum while x_- is a minimum. For $\sigma^2 = \sigma_c^2$, the two extrema degenerate to form an inflection point with horizontal tangent. For $\sigma^2 > \sigma_c^2$, finally, extrema do not occur and p_s is a monotonically decreasing function of $\tilde{\rho}$. These qualitative changes of the probability distribution are illustrated by the insets of Fig. 1.

For $\sigma^2 = \sigma_c^2$, the present model system undergoes a noise-induced phase transition. This is visualized in Fig. 2 showing a family of probability distribution functions for $\phi = 0.3$ and $\sigma_c^2 \approx 1.404$, and different values of σ^2 . With increasing multiplicative noise the distribution functions are seen to depart from the deterministic value $\tilde{\rho} = 1$, become broad and accentuated at $\tilde{\rho} = 0$.† In the following section, the relation between this transition and the phenomenon of dislocation cell formation will be discussed in quantitative terms.

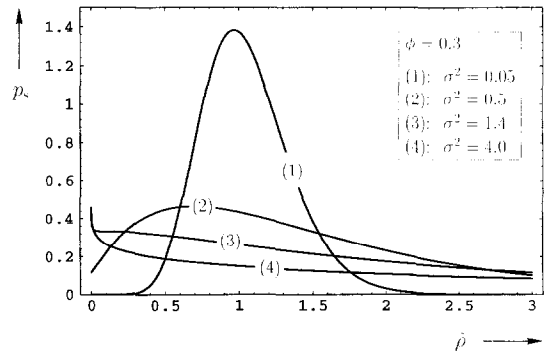


Fig. 2. Plots of the steady-state probability distribution function p_s as a function of the scaled dislocation density $\tilde{\rho}$ for several values of the noise intensity σ^2 and an additive noise parameter $\phi = 0.3$. Note that $\sigma^2 = 1.4$ [curve (3)] is close to the critical value $\sigma_c^2 \approx 1.404$.

†Note that for $\sigma^2 = 0.05$ and 0.5 the minimum is so close to $\tilde{\rho} = 0$ that it is not resolved in the plots of Fig. 2.

4. RESULTS AND DISCUSSION

The results of the preceding section do not refer directly to the physical space, but concern the system's evolution in probability space. As immediate evidence of dislocation patterning does not derive, we have to investigate the signature of cell formation with regard to the probability distribution of the dislocation density.

First of all it is interesting to note that the dislocation density distribution may deviate markedly from what is expected in deterministic terms for the steady-state dislocation density, namely

$$\tilde{\rho} = 1 \text{ or } \rho = \left(\frac{A \langle \tau^{\text{eff}}_i \rangle}{B_2 \langle \dot{\gamma} \rangle} \right)^2. \quad (40)$$

With increasing multiplicative noise, the probability distribution $p_s(\tilde{\rho})$ becomes peaked at $\tilde{\rho} = 0$, meaning that the system tends to reduce, in places, the dislocation density. At the same time, $p_s(\tilde{\rho})$ flattens out corresponding to a broad spectrum of possible dislocation densities, including densities much higher than average. This means that dislocation-poor and -rich states start coexisting. It is tempting to identify this with a preliminary stage of dislocation cells associated with the formation of heterogeneous dislocation entanglements. The accentuation at $\tilde{\rho} = 0$ corresponds to the appearance of dislocation free regions, that is the formation of *cell interiors*. Associated with the flattening of the distribution function is an increased probability of finding high dislocation density regions, that is *cell walls*. The broad extension of the distribution function indicates that a regular periodic cell structure with a uniform cell size does not evolve. This is in accordance with the observation of a broad spectrum of cell sizes corresponding to a hierarchical organization of cells, subcells etc. that was proposed to be fractal [18].

For a quantitative discussion of the present model, estimates for the parameters A , B_1 and B_2 can be derived from comparing the *macroscopic* dynamics of the constitutive equations (16)–(18) and (22) with the strain hardening observed experimentally. Let us assume that (i) most dislocations are immobile:

$$\rho_m \ll \rho_i \approx \rho, \quad \partial_t \rho_i = B_1 \sqrt{\rho} \langle \dot{\gamma} \rangle \approx \partial_t \rho; \quad (41)$$

(ii) dynamic recovery by annihilation is small compared to dislocation multiplication:

$$\partial_t \rho \approx A \tau^{\text{ext}} \langle \dot{\gamma} \rangle \quad (42)$$

[here equation (7) was used]; and (iii) the external resolved shear stress is governed by the long-range internal stresses

$$\tau^{\text{ext}} \approx \langle \tau^{\text{int}} \rangle = \alpha \mu b \sqrt{\rho}, \quad (43)$$

with a coefficient $\alpha \approx 0.3$. Comparison of equations (41) and (42) then gives

$$\frac{B_1}{A} = \alpha \mu b \quad (44)$$

and by integration of equation (42)

$$A = \frac{2h}{(\alpha \mu b)^2}, \quad B_1 = \frac{2h}{\alpha \mu b} \quad (45)$$

follows where

$$h = \frac{\partial \tau^{\text{ext}}}{\partial \langle \dot{\gamma} \rangle} \quad (46)$$

denotes the strain hardening coefficient. Moreover, we shall assume a 20% reduction of the stored dislocation density due to annihilation: $B_1/B_2 = 5$.

The control parameter of the additive noise, equation (26), may be approximated by

$$\phi = \frac{\langle \tau^{\text{eff}} \rangle}{\tau^{\text{ext}}}. \quad (47)$$

Provided that the Cottrell–Stokes law [19] holds, ϕ is constant during tensile deformation of a given material so that we can concentrate on the second model parameter, i.e. the noise intensity σ^2 . Combining equations (4), (7), (22), (24), (27) and (44) with $L = (B_1 \sqrt{\rho b})^{-1}$ for the slip length, supercritical fluctuations are predicted for

$$\frac{\langle \delta \dot{\gamma}^2 \rangle}{\langle \dot{\gamma} \rangle^2} > \left(\frac{B_1}{B_2} \right)^2 \frac{\rho}{\rho_m} \sigma_c^2(\phi) = 25 \frac{\rho}{\rho_m} \sigma_c^2. \quad (48)$$

With the relation (10) for the strain-rate fluctuations and $\rho/\rho_m = 10$ and $B_1/B_2 = 5$, this condition can also be written as

$$\frac{\langle \tau^{\text{int}} \rangle}{S} > \left(\frac{B_1}{B_2} \right)^2 \frac{\rho}{\rho_m} \sigma_c^2 = 250 \sigma_c^2. \quad (49)$$

From equations (48) and (49), interesting conclusions derive.

- (1) Dislocation cell formation is favored if (i) strain-rate fluctuations are large due to a small strain-rate sensitivity (large activation volume); (ii) a high fraction of dislocations is mobile; (iii) annihilation is efficient (B_1/B_2 small); and (iv) the effective stress contribution is high (large ϕ , small σ_c^2).
- (2) With $\langle \tau^{\text{int}} \rangle/S \approx 4 \times 10^2$ as a typical value of a f.c.c. metal [20, 21], the condition (49) is met for $\sigma_c^2 = 1.6$ corresponding to $\phi = 0.2$. This is a reasonable order of magnitude estimate which could explain why dislocation cells are readily formed in f.c.c. metals.
- (3) In b.c.c. metals deformed below the transition temperature T_c , thermal glide is controlled by the Peierls stress. Owing to a small activation volume, this gives rise to a high strain-rate sensitivity—typically one or two orders of magnitude larger than in the f.c.c. case. Even for $\phi = 1$ corresponding to $\sigma_c^2 \approx 0.7$, the condition (49) is far from being satisfied. So the present theory can qualitatively explain why cellular dislocation structures are either absent below

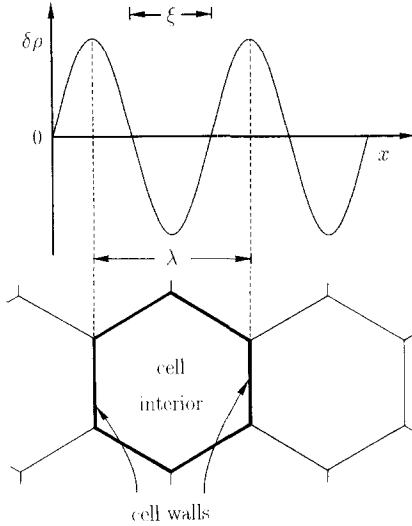


Fig. 3. Motivation of equation (51) relating the dislocation cell size λ to the correlation length ξ . The spatial variations of the total dislocation density are schematically depicted in the upper part.

T_c [4], or why cell formation is more retarded the lower the deformation temperature [22].

Although the criterion (49) can reproduce important experimental trends, one may miss the intuitive background of this result. Let us therefore formulate condition (49) in terms of the correlation length ξ introduced in Section 2. Combining equations (15), (43) and (49), the condition for cell formation reads

$$\xi > \frac{\sigma_c}{4\pi\alpha} \frac{B_1}{B_2} \rho_m^{-1/2}. \quad (50)$$

Using again $B_1/B_2 = 5$, $\sigma_c = 1.6$, $\alpha = 0.3$, dislocation cells are predicted for $\xi > 1.7\rho_m^{-1/2}$, i.e. if the correlation length is of the order of, or larger than, the average distance between mobile dislocations. This result indicates that cell formation is primarily due to correlated dislocation glide, whereas dislocation relaxation into configurations of lower elastostatic energy represents a secondary consequence. Interpreted as a collective phenomenon, the difficulty of cell formation in b.c.c. metals may be attributed to a correlation length ξ being too small (large S) for collective glide.

It is natural to assume that the correlation length of dislocation dynamics is passed on the coherence length of dislocation patterning. This leads us to identifying 2ξ with the average dislocation cell size λ (c.f. Fig. 3):

$$\lambda \approx 2\xi = \frac{\mu b}{2\pi\sqrt{\alpha\mu b S}\sqrt{\rho}}. \quad (51)$$

Again, this scaling relation indicates the importance of the strain-rate sensitivity. As S is a *dynamic* response function, equation (51) reflects the idea that cell formation is a dynamic process far from equilibrium. With $\mu = 5 \times 10^4$ MPa, $b = 2.5 \times 10^{-10}$ m, $\langle\tau^{\text{int}}\rangle = 30$ MPa and $S = 2.5 \times 10^{-3}\langle\tau^{\text{int}}\rangle$, a cell

size $\lambda \approx 1.3\mu\text{m}$ derives which agrees within 30% accuracy with experimental findings on $\langle 100 \rangle$ oriented Cu single crystals [23].

A central question is associated with the physical origin of the empirical “principle of similitude”, equation (1). According to equation (51), this scaling law can be understood in terms of any process that gives rise to a Cottrell–Stokes law [19] with $S \sim \langle\tau^{\text{int}}\rangle = \alpha\mu b\sqrt{\rho} \sim \tau^{\text{ext}}$, i.e. if dislocation–dislocation interactions prevail over interactions with other defects and over the lattice friction. Taking $S = 2.5 \times 10^{-3}\langle\tau^{\text{int}}\rangle$, $\langle\tau^{\text{int}}\rangle \approx \tau^{\text{ext}} = \sigma^{\text{ext}}/M$, with an orientation factor $M = \sqrt{6}$, equation (1) is recovered with $K_1 \approx 8$ and $m = 1$. This is in satisfactory agreement with compilations of experimental data yielding mean values $K_1 \approx 10$ [24] and $K_1 \approx 20$ [6], respectively. On the other hand, a detailed experimental check of equation (51) is difficult, just because the strain-rate sensitivity dependence of the cell size is masked by the Cottrell–Stokes law. Therefore, it is suggested to compare equation (51) with dislocation dynamical simulations, where S can be treated as an input parameter [23].

As to single-glide oriented crystals, the Cottrell–Stokes law was observed to hold at (i.e. the ratio $\langle\tau^{\text{int}}\rangle/S$ is not affected by) the transition from stage II to III [25, 26]. Here dislocation patterning starts in the late stage II by the formation of heterogeneous entanglements, while well-developed dislocation cells do not develop before stage III [2]. As stage III is commonly associated with cross slip, we comment on its role in the present theory. The constitutive equations (16)–(18) are based on dynamic recovery by annihilation without making reference to geometrical details of this process. The onset of abundant cross slip in stage III is expected to lead to a sharp decrease of B_1/B_2 in such a way that the condition (48) is suddenly met. This offers an explanation why cell formation occurs within a relatively small interval of strain at the transition from stage II to III. This is to be distinguished from multiple slip, where dislocation cells emerge gradually at comparatively low strains. This compares well with the present ideas according to which a smooth transition is expected from the sequence of distribution functions plotted in Fig. 2.

Staker and Holt observed that by increasing the impurity content of various materials, the cell size for a given dislocation density is lowered [24]. They attributed this observation to an increased “friction stress” which should lead to a smaller dislocation interaction distance governing the cell size. This idea fits well with the present theory if this interaction distance is identified with the correlation length [equation (15)] which is, in fact, decreasing with increasing friction (expressed by S).

Some general remarks on the principal differences between the present stochastic dislocation dynamics and the thermodynamic approach to dislocation patterning might be instructive. Although dislocation

cells represent a "low energy dislocation structure", inasmuch as long-range interactions are partially screened by entanglements, they are not believed to form according to an energetic principle, because far-from equilibrium conditions are steadily maintained by plastic deformation. We rather believe cell formation to result from an evolutionary process. The geometrically necessary effective stress fluctuations experienced by gliding dislocations cause appreciable fluctuations of the local strain rate [equation (12)]. This enables the mobile dislocations to probe again and again new configurations (comparable to mutations in the evolution of life). During this process, energetically favorable configurations possess a certain chance to become stabilized (comparable to selection), whereas unfavorable arrangements are rapidly dissolved again. While cross slip and climb support this process by increasing the "selection pressure", the very driving force is due to the intrinsic strain-rate fluctuations maintained by the external mechanical work.

5. CONCLUSIONS

The present analysis indicates that a stochastic dislocation dynamics theory represents a valuable tool for describing dislocation patterning on a mesoscopic scale. By applying this approach to the formation of dislocation cells in multiple slip, some fundamental observations could be explained:

- a physical interpretation of the inverse proportionality of the cell size and the flow stress was obtained (law of similitude);
- conditions for cell formation derived, in particular, the difficulty of cell formation in b.c.c. metals deformed below the transition temperature was explained;
- the role of cross slip in facilitating cell formation was clarified.

The results may shed new light on fundamental aspects of dislocation dynamics. In particular, cell formation can be attributed to an evolutionary process driven by intrinsic fluctuations, with the strain-rate sensitivity acting as a control parameter.

REFERENCES

1. L. P. Kubin, in *Treatise in Materials Science and Technology* (edited by H. Mughrabi), p. 137. VCH, Weinberg (1993).
2. C. Schwink, *Scripta metall. mater.* **27**, 963 (1992).
3. F. Louchet and Y. Brechet, *Solid State Phenom.* **3&4**, 335 (1988).
4. A. Luft, *Prog. Mater. Sci.* **35**, 97 (1991).
5. N. Hansen and D. Kuhlmann-Wilsdorf, *Mater. Sci. Engng* **81**, 141 (1986).
6. S. V. Raj and G. M. Pharr, *Mater. Sci. Engng* **81**, 217 (1986).
7. G. Saada, *Acta metall.* **8**, 200 and 841 (1960).
8. D. L. Holt, *J. appl. Phys.* **41**, 3197 (1970).
9. D. Walgraef and E. C. Aifantis, *Int. J. Engng Sci.* **23**, 1351 (1985).
10. J. Kratochvil, *Scripta metall. mater.* **24**, 891 and 1225 (1990).
11. P. Hähner, *Appl. Phys. A*, in press.
12. M. Wilkens, *Acta metall.* **17**, 1155 (1969).
13. C. Schwink and E. Göttler, *Acta metall.* **24**, 173 (1976).
14. P. Hähner, *Appl. Phys.* **A58**, 49 (1994).
15. U. F. Kocks, *J. Engng Mater. Technol.* **98**, 76 (1976).
16. W. Horsthemke and R. Lefever, *Noise-Induced Transitions*. Springer, Berlin (1984).
17. H. Haken, *Advanced Synergetics*. Springer, Berlin (1987).
18. J. Gil Sevillano, E. Bouchaud and L. P. Kubin, *Scripta metall. mater.* **25**, 355 (1991).
19. F. R. N. Nabarro, *Acta metall. mater.* **38**, 161 (1990).
20. S. J. Basinski and Z. S. Basinski, in *Dislocations in Solids*, Vol. 4 (edited by F. R. N. Nabarro), p. 261. North-Holland, Amsterdam (1979).
21. U. F. Kocks, A. S. Argon and M. F. Ashby, *Thermodynamics and Kinetics of Slip*, *Progress Materials Science*, Vol. 19, p. 259. Pergamon, Oxford (1975).
22. A. S. Keh and S. Weissmann, in *Electron Microscopy and Strength of Crystals* (edited by G. Thomas and J. Washburn), p. 231. Interscience Publishers, New York (1963).
23. L. P. Kubin, G. Canova, M. Condat, B. Devincre, V. Pontikis and Y. Brechet, *Solid State Phenom.* **23&24**, 455 (1992).
24. M. R. Staker and D. L. Holt, *Acta metall.* **20**, 569 (1972).
25. P. R. Thornton, T. E. Mitchell and P. B. Hirsch, *Phil. Mag.* **7**, 337 (1961).
26. F. R. N. Nabarro, in *Proc. of the 7th Int. Conf. on the Strength of Metals and Alloys (ICSMA 7)* (edited by H. J. McQueen et al.), Vol. 3, p. 1667. Pergamon, Oxford (1985).